

SHADING WITHOUT SHAPE FOR TRN MAP GENERATION

Yang Cheng*, Adnan Ansar, Zachary Morgan; Jet Propulsion Laboratory, 4800 Oak Grove Dr, Pasadena, CA 91109
*ycheng@jpl.nasa.gov

Abstract. We present a novel approach to preparing terrain relative navigation maps for lunar lander missions. The approach, called *image Shading Without Shape (SWS)*, can produce high quality TRN maps at the native resolution of LRO NAC imagery. Compared to traditional methods, such as *shape from shading* or *stereo photogrammetry*, this approach is simpler, faster and more accurate.

Introduction. NASA’s Human Landing System (HLS) program is developing ground breaking technology to send crewed spacecraft to the lunar south pole, where many highly desired scientific sites are located. Terrain Relative Navigation (TRN) is among the most critical technologies to allow a spacecraft to land precisely and safely at these sites. The onboard TRN system carries a precomputed terrain map of the landing site, and then descent imagery is matched to the reference map to localize the spacecraft attitude and position with respect to this reference map. Mars 2020 was the first mission which used TRN and an on-board map to land the Perseverance rover successfully in Jezero crater [1]. However, the south pole of the Moon presents numerous challenges to a TRN system. First, because of extreme low sun elevation and a wider range of sun azimuth angles, the surface appearance changes dramatically over time. Orbital imagery is less likely to exist with lighting conditions matching the time of landing. Therefore, a TRN map has to be created by rendering an appearance map using an existing DEM and the expected lighting angle at the time of landing. This requires a high resolution, high fidelity DEM. However, since all orbital assets for the moon are in polar orbits, it is very difficult to acquire stereo imagery with the correct geometry to construct high resolution DEMs using traditional photogrammetry. Thus, the only viable solution to create a high quality DEM is *shape from shading (SFS)* [2]. However, SFS is computationally expensive, since it involves a series of large nonlinear optimizations and often needs manual parameter adjustment during a run. In this paper we propose an alternative solution, which bypasses the expensive 3D reconstruction step, whether stereo or SFS, and directly models the image intensity as a function of sun vector at each pixel. We call this method *Shading Without Shape (SWS)*. The assumptions of SWS are as follows:

1. For each point in the mapped area, there are at least four images. The Narrow Angle Cameras (NAC) aboard NASA’s Lunar Reconnaissance Orbiter (LRO) have collected a large volume of images, particularly over both poles. Often as many as 10s even 100s of images can be found for a given

location. Figure 1 shows sun angles at a potential landing site and the count of the NAC images available at this site.

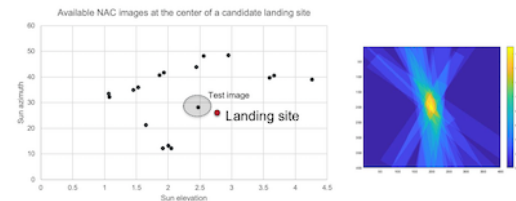


Figure 1. Sun angles associated with NAC images near a potential landing site (Left). Image count (Right).

2. A coarse resolution and lower quality DEM is available. Fortunately, The LRO Lunar Orbiter Laser Altimeter (LOLA) team has produced up to 5m/pixel DEMs over both poles.
3. The TRN system uses the terrain appearance rather than elevation data for terrain matching. In this case the image resolution, horizontal accuracy and appearance are more important than the vertical information. We assume the existing DEM is sufficient for the TRN solution. Furthermore, because TRN matches discrete points and employs outlier rejection, the process is robust to some fraction of bad points or holes in the map.

SWS contains four major components:

Image Selection. For a given landing site and time, we select a set of NAC images over the landing site. The selection criteria include the image footprint and the sun angles.

Image Alignment (IA). The key procedure is to align all images precisely into the same coordinate frame. Often times, both the Spacecraft orbit determination (S/C OD) solution and pointing solution are not sufficiently accurate to align the input images to the pixel level. The objective of IA is to mitigate these errors. Unlike the method proposed in [2], where the image alignment is done on a map projection frame, we execute IA on the local Cartesian frame [3], which is computationally easier. Since the mapping from this local Cartesian frame to the body frame is a rigid 3d transformation, there is no loss of generality. IA contains three individual steps:

- The OD solution selection. There are two OD solutions available, LROC SPK and LOLA SPK. After careful evaluation, we found the LOLA SPK provides a better OD solution[4].

- Similar to MRO CTX imagery, we found the time tags of NAC images contain relative time offsets. We use the method in [1] to correct the offsets (fig 2).

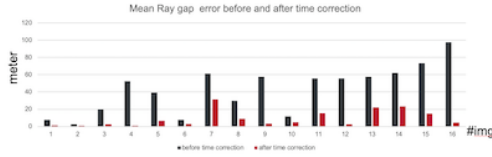


Figure 2: The time correction can significantly reduce the image misalignment. The remaining misalignments are mainly caused by pointing error.

- Finally, we correct the pointing error. Due to the low convergence angles among the input NAC images, traditional bundle adjustment (BA) results in large errors along the line of sight. We use the existing DEM to constrain the range for 3d triangulation and better condition BA. Then we adjust the camera pointing using the method in [1]. After IA, the image can be aligned in general to less than one pixel of registration error (fig 3).

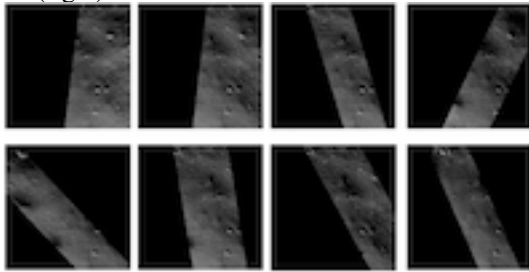


Figure 3. Aligned and rectified NAC images.

Image Intensity Modeling. The IA process above allows us to project all input images into the same frame. Misalignment in general is less than one pixel. Like the SFS method, a pixel is observed multiple times (I_1, I_2, \dots, I_n) and the corresponding sun elevations and azimuths are known. The sun vector in the local Cartesian frame can be calculated $S(V_{xi}, V_{yi}, V_{zi})$ for $i = 1, 2, 3, \dots, n$.

Assume the image intensity is a linear function of sun vector (V_x, V_y, V_z)

$$I = aV_x + bV_y + cV_z + d$$

Then the (a, b, c, d) can be determined by a least squares solution at each pixel location.

TRN image Generation. Once (a, b, c, d) is determined, for an any given sun angles, the intensity can be calculated. Fig 4 shows a rendered image (left) using the formula above and a real NAC image (right) under the same sun illumination conditions.

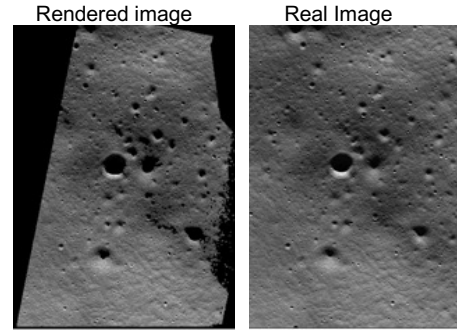


Figure 4. Synthetic image vs the real NAC image.

We compared the horizontal difference between the synthetic image the real image. The pixel motion is less than 0.66 pixel 3 sigma in both x and y directions, and a typical correlation score of greater than 0.7 indicates high match confidence (fig 5). This performance is significantly better than for any maps prepared by other approaches. The high correlation score indicates the synthetic image is a faithful representation of the terrain appearance and that it could be used in-flight for TRN.

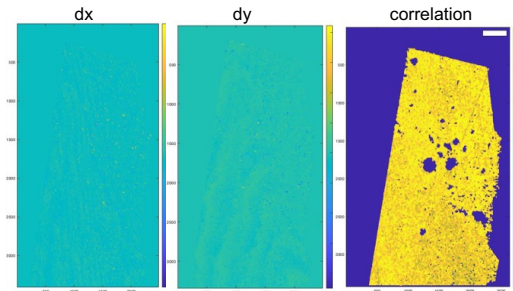


Figure 5: The delta map and correlation score between the real NAC images and synthetic image.

Conclusions. We offer SWS as a simple and effective method for rendering the TRN map for future lunar lander missions. Under the assumed conditions, this approach is able to produce high quality maps which we expect to satisfy flight mission requirements.

Acknowledgement. This research was carried out at the Jet Propulsion Laboratory, California Institute of Technology, under a contract with the National Aeronautics and Space Administration. © California Institute of Technology.

[1] Cheng, Y., Ansar, A., & Johnson, A. (2021). Making an onboard reference map from MRO/CTX imagery for Mars 2020 Lander Vision System. *Earth and Space Science*, 8, e2020EA001560.
 [2] Alexandrov, O., & Beyer, R. A. (2018). Multiview shape-from-shading for planetary images. *Earth and Space Science*, 5, 652–666
 [3] Andrew Johnson et al, Mars2020 Lander Vision System Flight Performance, SciTech 2022 Forum.
 [4] Barker, M.K., et al. (2021), Improved LOLA Elevation Maps for South Pole Landing Sites: Error Estimates and Their Impact on Illumination Conditions, *Planetary & Space Science*, Volume 203, 1 September 2021, 105119